Optimal Parameter Setting of FACTS Devices

V. Srinivasa Rao, R. Srinivasa Rao

Abstract: Flexible AC transmission system (FACTs) controllers are widely used for better utilization of existing transmission network. Important step after finding the optimal location of FACTs device in power system is to determine its optimal parameters. In this paper, optimal parameter setting of FACTs devices has been carried out. Newton- Raphson (NR) power flow technique with power flow limits on the specified lines is used to determine the optimal parameters of the FACTs devices. FACTs devices considered here are, TCSC, TCPAR and UPFC. The models of FACTs devices are presented and analyzed. The algorithm is implemented on standard 5 bus and 14 bus systems. Severity of the system loading is described by real power flow Performance Index (PI). Power loss and Performance Index values before and after placing the FACTs device have been compared. It is observed that, for 5 Bus system, after placement of TCSC and TCPAR, the performance index is reduced but, power loss is slightly increased. But, in the case of UPFC, both performance index and real power loss have been reduced. For 14 Bus System, with all devices, PI values have reduced and active power loss is slightly increased. In all the test systems, it is observed that power flows have been controlled as per the limits specified and voltage profile has been improved.

Keywords: FACTs devices, parameter setting, placement of FACTs devices, Performance Index, real power loss.

I. INTRODUCTION

To meet the load demands in a power system and to improve the stability and reliability, the existing power system must be utilized more efficiently. Electric Power Systems are operated close to their stability limits due to several problems associated with transmission network expansion. The purpose of the transmission network is to supply the load at a required reliability and maximum efficiency at a lower cost. Increase in power demand results in heavy line flows, greater losses, and may threaten system security and stability. Hence, there is a need for utilizing available power system capacities effectively by installing new devices such as FACTs [1]. The concept of FACTs was first introduced by N.G. Hingorani in 1988 [2] at Electric power research institute (EPRI), USA. The application of FACTs is intended for the improvement of stability, Control of power flow, voltage profile management, loss minimization and power factor improvement.

Variable series capacitors, unified power flow controllers and phase shifting transformers can be utilized to change the power flow by changing the parameters of transmission line [3].

V. Srinivasa Rao is currently working as Associate Professor in the Department of EEE, Aditya Engineering College, Surampalem, India.
Email: connectvsr@gmail.com, Cell: +919440504272
Dr. R. Srinivasa Rao is currently working as Professor in the Department of EEE, University College of Engineering, JNTUK, Kakinada, India.
Email:srinivas.jntueee@gmail.com.

FACTs devices offer new control mechanism for both steady state and dynamic state of the power system operation [4]-[5]. Using controllable series capacitors, minimized losses and increased stability margin can be attained in the line flows without violating thermal limits. The FACTS devices have become cost effect because of the developments in power electronics [6]-[7]. The location for placement of FACTS devices is important because of its high investment.

There are various approaches proposed in the literature for optimizing location and parameter setting of the FACTs devices from various viewpoints [8]-[10]. Sensitivity indices based on line loss have been developed for placement of series capacitors in [11]. Other researchers considered the use of FACTs devices for transmission congestion management purposes in [12]-[14]. Optimal locations to place TCSC was determined using the tangent vector technique [15]. The placement of TCSC and TCPAR can be decided on the basis of reducing losses in the absence of congestion [16]-[19]. Although TCSC introduces new power system dynamics that must be analyzed by the system protection engineer, but in the very limited works presented [20]–[23], the transient process of TCSC is not modeled and the TCSC is simply considered as a linear component with nonlinear limits. In [20], TCSC is being operated with a 10% vernier setting prior to the fault, and thyristors are operated in the bypass mode during the fault. The study did not encompass the relay performance during TCSC modulation. In [21], it is assumed that only the open loop impedance control mode is embedded in the TCSC control system and as a result, the firing angle could be taken as one of the inputs to the ANN-based relay. In [22], the equations to determine the line impedance to the fault are derived based on the TCSC bypass mode assumption during the fault. In [23], the influence of the sampling frequency on the distance protection performance is mainly considered.

UPFC combines properties of series and shunt controllers. It is a two-converter series- shunt FACT controller which has better power flow and voltage control capability than one-converter FACTs controller. The UPFC [24] is one of the most promising FACTs devices for load flow control since it can either simultaneously or selectively control active and reactive power flow along the lines as well as the nodal voltages. The multi objective evolutionary algorithm (EA) has been applied to optimal location and parameters of the UPFC [25] and thyristor-controlled phase-shifting transformer [26] in order to minimize real power loss and to improve voltage profile. A parallel Tabu search based placement of UPFC for enhancement of Available Transfer Capability (ATC) has been proposed in [27]. Lima et al. [28] proposed optimal number, location, and control settings of phase shifters to increase system loadability using mixed integer linear programming (MILP). UPFC is placed to improve the transfer capability in the transmission systems [29].

In this paper, the optimal parameter setting s of TCSC, TCPAR and UPFC have been obtained separately, using N-R polar with limits on specified lines.

The rest of the paper is organized in the following way. Section II consists of mathematical modeling of TCSC, TCPAR and UPFC. Section III consists of simulation results. Conclusions are presented in Section IV.

II. MATHEMATICAL MODELING OF FACTS DEVICES

A. Thyristor Controlled Series Compensator (TCSC)

The TCSC power flow model presented in this section is based on the simple concept of variable series compensation, the value of which is adjusted automatically to constrain the power flow across the branch to a specified value [30, 31]. The reactance X_c, shown in Figure 1, represents the equivalent reactance of all the series-connected modules making up the TCSC, when operating in either the inductive or the capacitive regions.

A transmission line connected between bus-i and bus-j with a TCSC is shown in Fig. 1, although the transmission line is not shown. In Fig .1, V_i, V_j are complex voltages at buses i, j, respectively. They can be further defined as $V_n=V_n\angle\theta_n$ (n=i, j) and V_n, θ_n are the magnitude and angle of V_n respectively. TCSC is considered as static reactance during steady state X_c. The real and reactive power flow at bus i and j of a line having series impedance $Z_c= jX_c$ can be derived as:

$$P_i = V_i V_j B_{ij} \sin(\delta_i - \delta_j) \quad (1)$$

$$Q_i = -V_i^2 B_{ii} - V_i V_j B_{ij} \cos(\delta_i - \delta_j) \quad (2)$$

$$P_j = V_j V_i B_{ji} \sin(\delta_j - \delta_i) \quad (3)$$

$$Q_j = -V_j^2 B_{jj} - V_j V_i B_{ji} \cos(\delta_j - \delta_i) \quad (4)$$

Where, $B_{ij} = \frac{1}{Z_c} = B_{ji}$ and $B_{ii} = -\frac{1}{Z_c} = B_{jj}$

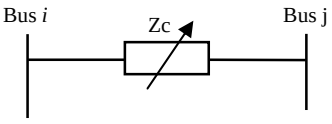

Fig. 1. Transmission line model with TCSC

a) Operating constraints of TCSC

The equivalent reactance of the TCSC are constrained by

$$X_c^{\min} \le X_c \le X_c^{\max} \quad (5)$$

Where $X_c^{\min}$, $X_c^{\max}$ are minimum and maximum reactance limits of X_c, respectively

b) Implementation of TCSC in Newton power flow

The Fig.1 shows the way of implementation of the TCSC in Newton- Raphson load flow algorithm [32, 33]. The FACTs branch i-j, active power flows P^c_{ij} can be controlled to match with the reference P_{ij}^{spec}. P^c_{ij} is the calculated power as given by equation (1). The active power balance at buses i, j should be maintained. The Newton power flow equation with incorporation of TCSC is written as in equation (6).

Where $\Delta P_i, \Delta P_j, \Delta Q_i, \Delta Q_j$ are the active and reactive power mismatches at buses i, j, respectively. P_i, P_j, Q_i, Q_j are the active and reactive power flows leaving the buses i, j, respectively. In this formulation, the terms of the first four rows of the system Jacobian matrix relate directly to the power mismatch equations , while the last row of the Jacobian matrix corresponds to the TCSC power flow control at buses i, j. The elements of Jacobian matrix are given in the Appendix.

$$\begin{pmatrix} \Delta P_i \\ \Delta P_j \\ \Delta Q_i \\ \Delta Q_j \\ P_{ij}^{spec} - P_{ij}^c \end{pmatrix} = \begin{pmatrix} \frac{\partial P_i}{\partial \delta_i} & \frac{\partial P_i}{\partial \delta_j} & \frac{\partial P_i}{\partial V_i}V_i & \frac{\partial P_i}{\partial V_j}V_j & \frac{\partial P_i}{\partial X_c}X_c \\ \frac{\partial P_j}{\partial \delta_i} & \frac{\partial P_j}{\partial \delta_j} & \frac{\partial P_j}{\partial V_i}V_i & \frac{\partial P_j}{\partial V_j}V_j & \frac{\partial P_j}{\partial X_c}X_c \\ \frac{\partial Q_i}{\partial \delta_i} & \frac{\partial Q_i}{\partial \delta_j} & \frac{\partial Q_i}{\partial V_i}V_i & \frac{\partial Q_i}{\partial V_j}V_j & \frac{\partial Q_i}{\partial X_c}X_c \\ \frac{\partial Q_j}{\partial \delta_i} & \frac{\partial Q_j}{\partial \delta_j} & \frac{\partial Q_j}{\partial V_i}V_i & \frac{\partial Q_j}{\partial V_j}V_j & \frac{\partial Q_j}{\partial X_c}X_c \\ \frac{\partial P_{ij}^c}{\partial \delta_i} & \frac{\partial P_{ij}^c}{\partial \delta_j} & \frac{\partial P_{ij}^c}{\partial V_i}V_i & \frac{\partial P_{ij}^c}{\partial V_j}V_j & \frac{\partial P_{ij}^c}{\partial X_c}X_c \end{pmatrix} \begin{pmatrix} \Delta\delta_i \\ \Delta\delta_j \\ \frac{\Delta V_i}{V_i} \\ \frac{\Delta V_j}{V_j} \\ \frac{\Delta X_c}{X_c} \end{pmatrix} \quad (6)$$

B. Thyristor Controlled Phase Angle Regulator (TCPAR)

Static model of TCPAR and transmission line [34] between bus *i* and bus *j* is shown in Fig. 2.

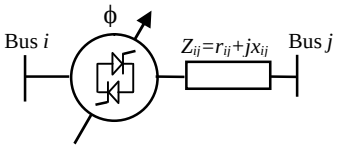

Fig. 2. TCPAR Equivalent circuit

a) Power flow equations of TCPAR

According to the equivalent circuit of the TCPAR shown in Fig. 2, the power flow equations at bus i and j can be derived as

$$P_i = V_i^2 G_{ii} - V_i V_j [G_{ij} \cos(\delta_i - \delta_j - \phi) + B_{ij} \sin(\delta_i - \delta_j - \phi)] \quad (7)$$

$$Q_i = -V_i^2 B_{ii} - V_i V_j [G_{ij} \sin(\delta_i - \delta_j - \phi) - B_{ij} \cos(\delta_i - \delta_j - \phi)] \quad (8)$$

$$P_j = V_j^2 G_{jj} - V_i V_j [G_{ji} \cos(\delta_j - \delta_i - \phi) + B_{ji} \sin(\delta_j - \delta_i - \phi)] \quad (9)$$

$$Q_j = -V_j^2 B_{jj} - V_i V_j [G_{ji} \sin(\delta_j - \delta_i - \phi) - B_{ji} \cos(\delta_j - \delta_i - \phi)] \quad (10)$$

b) Operating constraints of TCPAR

The phase angle shift of the TCPAR are constrained by

$$\phi^{\min} \le \phi \le \phi^{\max} \quad (11)$$

Where $\phi^{\min}$, $\phi^{\max}$ are minimum and maximum phase angle shift limits of ϕ, respectively

c) Implementation of TCPAR in Newton power flow

The Fig.2 shows the way of implementation of the TCPAR in Newton- Raphson load flow algorithm [35].

$$\begin{pmatrix} \Delta P_i \\ \Delta P_j \\ \Delta Q_i \\ \Delta Q_j \\ P_{ij}^{spec} - P_{ij}^s \end{pmatrix} = \begin{pmatrix} \frac{\partial P_i}{\partial \delta_i} & \frac{\partial P_i}{\partial \delta_j} & \frac{\partial P_i}{\partial V_i}V_i & \frac{\partial P_i}{\partial V_j}V_j & \frac{\partial P_i}{\partial \phi_{ij}} \\ \frac{\partial P_j}{\partial \delta_i} & \frac{\partial P_j}{\partial \delta_j} & \frac{\partial P_j}{\partial V_i}V_i & \frac{\partial P_j}{\partial V_j}V_j & \frac{\partial P_j}{\partial \phi_{ij}} \\ \frac{\partial Q_i}{\partial \delta_i} & \frac{\partial Q_i}{\partial \delta_j} & \frac{\partial Q_i}{\partial V_i}V_i & \frac{\partial Q_i}{\partial V_j}V_j & \frac{\partial Q_i}{\partial \phi_{ij}} \\ \frac{\partial Q_j}{\partial \delta_i} & \frac{\partial Q_j}{\partial \delta_j} & \frac{\partial Q_j}{\partial V_i}V_i & \frac{\partial Q_j}{\partial V_j}V_j & \frac{\partial Q_j}{\partial \phi_{ij}} \\ \frac{\partial P_{ij}^S}{\partial \delta_i} & \frac{\partial P_{ij}^S}{\partial \delta_j} & \frac{\partial P_{ij}^S}{\partial V_i}V_i & \frac{\partial P_{ij}^S}{\partial V_j}V_j & \frac{\partial P_{ij}^S}{\partial \phi_{ij}} \end{pmatrix} \begin{pmatrix} \Delta\delta_i \\ \Delta\delta_j \\ \frac{\Delta V_i}{V_i} \\ \frac{\Delta V_j}{V_j} \\ \Delta\phi_{ij} \end{pmatrix} \quad (12)$$

The FACTs branch i-j, P^s_{ij} can be controlled to match with the reference P_{ij}^{spec}. P^s_{ij} is the calculated power as given by equation (7). The Newton power flow equation with incorporation of TCPAR is written as in equation (12). In

this formulation, the terms of the first four rows of the system Jacobian matrix relate directly to the power mismatch equations, while the last row of the Jacobian matrix corresponds to the TCPAR power flow control at buses i, j.

C. Unified power flow controller (UPFC)

The model of UPFC is shown in Fig. 3, which represents the steady-state model. Fig. 3 consists of two ideal voltage sources that represent the switched voltage waveforms. The source impedances are included in the model. The ideal voltage sources are,

$$V_{cR} = V_{cR}(\cos\delta_{cR} + j\sin\delta_{cR}) \quad (13)$$

$$V_{vR} = V_{vR}(\cos\delta_{vR} + j\sin\delta_{vR}) \quad (14)$$

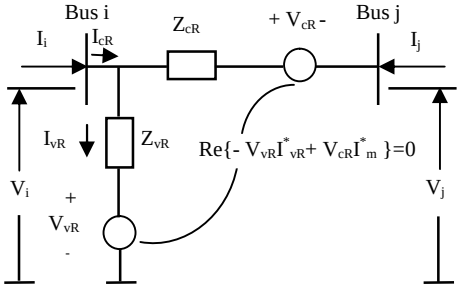

Fig.3. UPFC equivalent circuit

a) Power flow equations of UPFC

According to the equivalent circuit of the UPFC, the power flow equations can be derived as

At bus i:

$$\begin{aligned} P_i = {} & V_i^2 G_{ii} + V_i V_j [G_{ij}\cos(\theta_i - \theta_j) + B_{ij}\sin(\theta_i - \theta_j) \\ & + V_i V_{cR}[G_{ij}\cos(\theta_i - \phi_{cR}) + B_{ij}\sin(\theta_i - \phi_{cR}) \\ & + V_i V_{vR}[G_{ij}\cos(\theta_i - \phi_{vR}) + B_{ij}\sin(\theta_i - \phi_{vR}) \end{aligned} \quad (15)$$

$$\begin{aligned} Q_i = {} & -V_i^2 B_{ii} + V_i V_j [G_{ij}\sin(\theta_i - \theta_j) - B_{ij}\cos(\theta_i - \theta_j) \\ & + V_i V_{cR}[G_{ij}\sin(\theta_i - \phi_{cR}) - B_{ij}\cos(\theta_i - \phi_{cR}) \\ & + V_i V_{vR}[G_{ij}\sin(\theta_i - \phi_{vR}) - B_{ij}\cos(\theta_i - \phi_{vR}) \end{aligned} \quad (16)$$

At bus j:

$$\begin{aligned} P_j = {} & V_j^2 G_{jj} + V_i V_j [G_{ji}\cos(\theta_j - \theta_i) + B_{ji}\sin(\theta_j - \theta_i) \\ & + V_j V_{cR}[G_{jj}\cos(\theta_j - \phi_{cR}) + B_{jj}\sin(\theta_j - \phi_{cR}) \end{aligned} \quad (17)$$

$$\begin{aligned} Q_j = {} & -V_j^2 B_{ii} + V_i V_j [G_{ji}\sin(\theta_j - \theta_i) - B_{ji}\cos(\theta_j - \theta_i) \\ & + V_j V_{cR}[G_{jj}\sin(\theta_j - \phi_{cR}) - B_{jj}\cos(\theta_j - \phi_{cR}) \end{aligned} \quad (18)$$

Series converter:

$$\begin{aligned} P_{cR} = {} & V_{cR}^2 G_{ii} + V_i V_{cR}[G_{ij}\cos(\phi_{cR} - \theta_i) + B_{ij}\sin(\phi_{cR} - \theta_i) \\ & + V_j V_{cR}[G_{jj}\cos(\phi_{cR} - \theta_j) + B_{jj}\sin(\phi_{cR} - \theta_j) \end{aligned} \quad (19)$$

$$\begin{aligned} Q_{cR} = {} & -V_{cR}^2 B_{jj} + V_i V_{cR}[G_{ij}\sin(\phi_{cR} - \theta_i) - B_{ij}\cos(\phi_{cR} - \theta_i) \\ & + V_j V_{cR}[G_{jj}\sin(\phi_{cR} - \theta_j) - B_{jj}\cos(\phi_{cR} - \theta_j) \end{aligned} \quad (20)$$

Shunt converter:

$$P_{vR} = -V_{vR}^2 G_{vR} + V_i V_{vR}[G_{vR}\cos(\phi_{vR} - \theta_i) + B_{vR}\sin(\phi_{vR} - \theta_i) \quad (21)$$

$$Q_{vR} = V_{vR}^2 B_{vR} + V_i V_{vR}[G_{vR}\sin(\phi_{vR} - \theta_i) - B_{vR}\cos(\phi_{vR} - \theta_i) \quad (22)$$

Where,

$G_{ii} + jB_{ii} = \frac{1}{Z_{cR}} + \frac{1}{Z_{vR}}$, $G_{jj} + jB_{jj} = \frac{1}{Z_{cR}}$, $G_{ij} + jB_{ij} = -\frac{1}{Z_{cR}}$ and $G_{vR} + jB_{vR} = -\frac{1}{Z_{vR}}$

b) Operating constraints of UPFC

The equivalent controllable injected voltage source magnitudes and angles of the series and shunt converter are constrained by

$$V_{cR}^{\min} \le V_{cR} \le V_{cR}^{\max} \quad (23)$$

$$0 \le \theta_{cR} \le 2\pi \quad (24)$$

$$V_{vR}^{\min} \le V_{vR} \le V_{vR}^{\max} \quad (25)$$

$$0 \le \theta_{cR} \le 2\pi \quad (26)$$

Where $V_{cR}^{\min}$, $V_{vR}^{\min}$, $V_{cR}^{\max}$ and $V_{vR}^{\max}$ are minimum and maximum voltage limits of V_{cR} and V_{vR} respectively. The power balance equation for active power exchange (P_E) between the converters through common DC link is given by

$$P_E = P_{vR} + P_{cR} = 0, \quad (27)$$

Where $P_{vR} = V_{vR}I^*_{vR}$ and $P_{cR} = V_{cR}I^*_m$ (28)

Where, I^*_{vR} and I^*_m are the conjugate of I_{vR} and I_m

c) Power flow control of UPFC

The UPFC shown in Fig. 3, can control active and reactive power flows of line j-i. The active and reactive power flows of the line ji, are denoted by P_{ji} and Q_{ji}. The active and power flow constraints are

$$P_{ji} - P_{ji}^{spec} = 0 \quad (29)$$

$$Q_{ji} - Q_{ji}^{spec} = 0 \quad (30)$$

Where, P_{ji}^{spec}, Q_{ji}^{spec} are the specified active and reactive power flow references, respectively, and P_{ji}, Q_{ji} are calculated powers as given by equations (17) and (18) respectively

d) Implementation of UPFC in Newton power flow

The compact form of Newton power flow [36] equation with incorporation of UPFC may be written as.

$$\begin{bmatrix} \Delta P_i \\ \Delta P_j \\ \Delta Q_i \\ \Delta Q_j \\ P_{ji}^{spec} - P_{ji} \\ Q_{ji}^{spec} - Q_{ji} \\ -P_E \end{bmatrix} = \begin{bmatrix} \frac{\partial P_i}{\partial \theta_i} & \frac{\partial P_i}{\partial \theta_j} & \frac{\partial P_i}{\partial V_{vR}}V_{vR} & \frac{\partial P_i}{\partial V_j}V_j & \frac{\partial P_i}{\partial \phi_{cR}} & \frac{\partial P_i}{\partial V_{cR}}V_{cR} & \frac{\partial P_i}{\partial \phi_{vR}} \\ \frac{\partial P_j}{\partial \theta_i} & \frac{\partial P_j}{\partial \theta_j} & 0 & \frac{\partial P_j}{\partial V_j}V_j & \frac{\partial P_j}{\partial \phi_{cR}} & \frac{\partial P_j}{\partial V_{cR}}V_{cR} & 0 \\ \frac{\partial Q_i}{\partial \theta_i} & \frac{\partial Q_i}{\partial \theta_j} & \frac{\partial Q_i}{\partial V_{vR}}V_{vR} & \frac{\partial Q_i}{\partial V_j}V_j & \frac{\partial Q_i}{\partial \phi_{cR}} & \frac{\partial Q_i}{\partial V_{cR}}V_{cR} & \frac{\partial Q_i}{\partial \phi_{vR}} \\ \frac{\partial Q_j}{\partial \theta_i} & \frac{\partial Q_j}{\partial \theta_j} & 0 & \frac{\partial Q_j}{\partial V_j}V_j & \frac{\partial Q_j}{\partial \phi_{cR}} & \frac{\partial Q_j}{\partial V_{cR}}V_{cR} & 0 \\ \frac{\partial P_{ji}}{\partial \theta_i} & \frac{\partial P_{ji}}{\partial \theta_j} & 0 & \frac{\partial P_{ji}}{\partial V_j}V_j & \frac{\partial P_{ji}}{\partial \phi_{cR}} & \frac{\partial P_{ji}}{\partial V_{cR}}V_{cR} & 0 \\ \frac{\partial Q_{ji}}{\partial \theta_i} & \frac{\partial Q_{ji}}{\partial \theta_j} & 0 & \frac{\partial Q_{ji}}{\partial V_j}V_j & \frac{\partial Q_{ji}}{\partial \phi_{cR}} & \frac{\partial Q_j}{\partial V_{cR}}V_{cR} & 0 \\ \frac{\partial P_E}{\partial \theta_i} & \frac{\partial P_E}{\partial \theta_j} & \frac{\partial P_E}{\partial V_{vR}}V_{vR} & \frac{\partial P_E}{\partial V_j}V_j & \frac{\partial P_E}{\partial \phi_{cR}} & \frac{\partial P_E}{\partial V_{cR}}V_{cR} & \frac{\partial P_E}{\partial \phi_{vR}} \end{bmatrix} \begin{bmatrix} \Delta\theta_i \\ \Delta\theta_j \\ \frac{\Delta V_{vR}}{V_{vR}} \\ \frac{\Delta V_j}{V_j} \\ \Delta\phi_{cR} \\ \frac{\Delta V_{cR}}{V_{cR}} \\ \Delta\phi_{vR} \end{bmatrix} \quad (31)$$

If the voltage at bus 'i' is satisfying the specified voltage limits, the third column of Equation (31) is replaced by partial derivatives of mismatch powers with respect to the nodal voltage magnitude V_i even though, the shunt controller of UPFC is placed at i^{th} node. The shunt voltage magnitude increment of the shunt source, ($\Delta V_{vR}/V_{vR}$) is replaced by the nodal voltage magnitude increment at bus i ($\Delta V_i/V_i$). The elements of Jacobian matrix are given in the Appendix.

e) UPFC initial conditions

At all load buses voltage of $1.0\angle 0^0$ pu is considered and for all generator buses voltage angle of 0^0 is assumed as starting condition. For the UPFC, initial estimates V_{cR}, θ_{cR}^0 and θ_{vR}^0 can be obtained by assuming lossless UPFC and coupling transformers and null voltage angles in equations (15)-(18).

f) Series source initial conditions

For specified nodal powers at bus j, the solutions of equations (17) and (18) are,

$$\theta_{cR}^{0} = arctan\left(\frac{P_{ji}^{spec}}{|C1|}\right) \quad (32)$$

$$V_{cR}^{0} = \left(\frac{X_{cR}}{V_j^0}\right)\sqrt{P_{ji(spec)}^2 + (C1)^2} \quad (33)$$

Where, $$C1 = Q_{ji}^{spec} \text{ if } V_j^0 = V_i^0 \quad (34)$$

$$C1 = Q_{ji}^{spec} - \frac{V_j^0}{X_{cR}}\left(V_j^0 - V_i^0\right) \text{ if } V_j^0 \neq V_i^0 \quad (35)$$

X_{cR} is the inductive reactance of the series source and the superscript 0 indicates initial value.

g) Shunt source initial conditions

An equation for initialising the voltage angle of UPFC shunt source can be obtained by substituting equations (19) and (21) into equation (27) and performing simple operations, we obtain,

$$\theta_{vR} = -\arcsin\left(\frac{(V_i^0 - V_j^0)V_{cR}^0 X_{cR}\sin(\theta_{cR}^0)}{V_{vR}^0 V_i^0 X_{cR}}\right) \quad (36)$$

Where, X_{vR} is the inductive reactance of the shunt source.

III. RESULTS

In this section, the optimal parameter settings of FACTs devices are obtained for standard 5 bus and 14 bus systems. The reduction in Real power flow performance index, active power loss, power flows before and after placing each device, voltage magnitudes, phase angles and optimal parameter settings of FACTs devices are presented in this section. Optimal locations for placing TCSC and TCPAR have been obtained for 5 Bus and 14 Bus systems in [39] and optimal location for placing UPFC for the two said systems is presented in [40] by the authors. The present work, parameter settings of FACTs devices is a continuation of the work carried out in [39] and [40].

A. 5-bus system

Five-bus system [37] shown in Figure 4 consists of three generator buses, two load buses and six transmission lines. The lines 1-2 and 1-4 have impedance of 0.002+j0.01 pu and

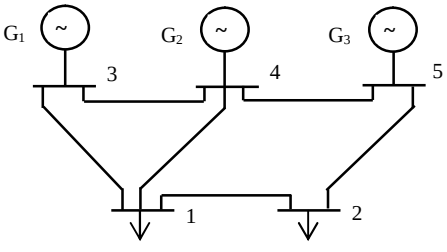

Fig. 4. Five bus system

shunt susceptance of 0.002pu each while other four lines have an impedance of 0.004+j0.02pu and shunt susceptance 0.004pu each. The base value is taken as 100MVA, line flow limit is set to be 800MW and bus 5 is considered as reference bus.

The original network has been modified to include a TCSC which compensates the transmission line connected between bus 2 and bus 5. An additional node, termed bus 6, is used to connect the TCSC. This is shown in Fig.5. The TCSC is used to divert the power flow in line number 3 which is above the specified limit of 8.0 pu to the line no. 4. The initial variable series compensation is set at 50% of the transmission line inductive reactance, i.e. X_c= -0.01 pu. Convergence was obtained in 6 iterations to a power mismatch tolerance of 1e-12.

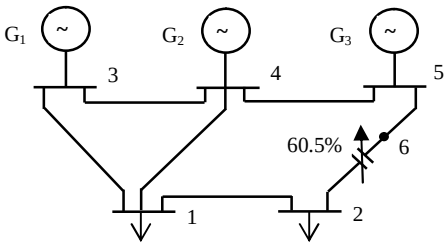

Fig. 5. Modified test system with TCSC

The original 5 bus network described in Fig.4 has been modified to include a TCPAR in series with the transmission line connected between bus 1 and bus 4 by an additional node, termed bus 6, as shown in Fig.6. The TCPAR is used to maintain active power flow from bus 6 towards bus 4 at 8.0 pu. The initial condition of the angle is zero. The primary and secondary winding impedances contain no resistance and an inductive reactance of 0.02 pu. The control of active power flow is achieved with the help of phase angle of the primary winding. Convergence was obtained in 6 iterations to a power mismatch tolerance of 1e-12. The TCPAR upheld its target value.

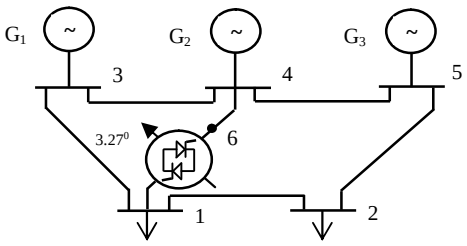

Fig. 6. Modified test system with TCPAR

The original network has been modified to include a UPFC which compensates the transmission line connected between bus 1 and bus 4.

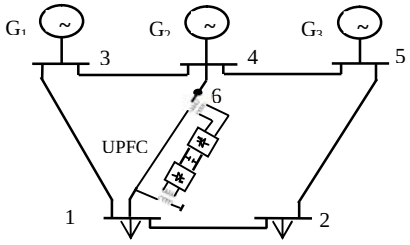

Fig.7. Modified test system with UPFC

An additional node, termed bus 6, is used to connect the UPFC. This is shown in Fig. 7. The UPFC is used to maintain active and reactive powers in the line no. 4, at 8.0 pu and 5 pu, respectively.

Moreover, the UPFC's shunt converter is set to regulate bus 1 voltage magnitude at 1 pu. The initial conditions of the UPFC voltage sources are computed by using equations (32)-(36) given in Section II, V_{cR} = 0.1238 pu, θ_{cR} = 37.16^0, V_{vR} = 1 pu and θ_{vR} = 0.0954^0 The source impedances have values of X_{cR}=X_{vR}=0.1 pu. Convergence was obtained in 6

iterations to a power mismatch tolerance of 1e-12. The UPFC upheld its target values.

The minimum and maximum limits of control parameters of FACT devices are presented in Table I for 5 bus system. Table II presents the optimal settings of the control parameters obtained with the help of N-R load flow solution.

TABLE I
Limits of control parameters of FACTS devices

FACTs Device/Control parameter	TCSC	TCPAR	UPFC
X_{min} (p.u)	-0.03	-	-
X_{max} (p.u)	0.03	-	-
ϕ_{min} (deg)	-	-10^0	-
ϕ_{max} (deg)	-	10^0	-
V_{cR}^{min} (p.u)	-	-	0.001
V_{cR}^{max} (p.u)	-	-	0.2
V_{vR}^{min} (p.u)	-	-	0.9
V_{vR}^{max} (p.u)	-	-	1.1

TABLE II
Optimal Setting of control parameters of FACTS devices

FACTs Device/Control parameter	TCSC	TCPAR	UPFC
X_C (p.u)	-0.0121	-	-
ϕ (deg)	-	3.27^0	-
θ_{cR} (deg)	-	-	32.0407^0
θ_{vR} (deg)	-	-	-4.4032^0
V_{cR} (p.u)	-	-	0.085
V_{vR} (p.u)	-	-	1.029

For TCSC, optimal setting of reactance is - 0.0121p.u. For TCPAR, optimal shift in phase angle is 3.27^0. Series injected voltage of UPFC is, V_{cR} is obtained as $0.085\angle 32.0407^0$ and voltage across the shunt converter is V_{vR} is obtained as $1.029\angle -4.4032^0$.

The optimal location for 5 bus system for each device is presented in the column 2 of Table III. Real power loss before and after placing each device is presented in column 5. Real power flow performance index before and after placing FACTs device is presented in Column 6. Percentage reduction in PI is presented in Column 7. It is observed that, for 5 Bus system, after placement of TCSC and TCPAR, the performance index is reduced but, power loss is slightly increased. But, in the case of UPFC, both performance index and real power loss have been reduced. Percentage reduction in PI is highest for TCSC with 23.28% and lowest in the case of UPFC with 15.21%.

TABLE III
Real power loss, real power flow PI and % Reduction in PI value

FACTs Device	L. No	From Bus	To Bus	Real Power Loss(p.u)	Performance Index (PI)	% reduction in PI value
System without any FACTs	-	-	-	0.5877	0.5614	-
TCSC	4	2	5	0.6038	0.4307	23.28
TCPAR	3	1	4	0.6343	0.4689	16.47
UPFC	3	1	4	0.5367	0.4760	15.21

Power flows before and after placing the three FACTs devices is presented in Table IV. Without any device, in 5 bus system, Line No.3 is observed to carry power flow of 8.97 pu. For the NR power flow algorithm, maximum power flow is specified as 8.0 pu on all lines. It is observed that in all the three cases, the power flow is restricted to 8.0 pu in line no. 3 after placing the devices.

TABLE IV
Power flow results with and without FACTS Device

L. No	Fr-To	Without FACTs		TCSC in line-4		TCPAR in line-3		UPFC in line-3	
		Pline	Ploss	Pline	Ploss	Pline	Ploss	Pline	Ploss
		(p.u)	(p.u)	(p.u)	(p.u)	(p.u)	(p.u)	(p.u)	(p.u)
1	1-2	0.963	0.0021	-0.2372	0.0038	0.4861	0.0027	0.5734	0.0016
2	1-3	-6.991	0.2214	-6.7635	0.1982	-7.4861	0.2900	-7.5734	0.2302
3	1-4	**-8.972**	0.2301	**-7.9993**	0.1771	**-8.0000**	0.1713	**-8.0000**	0.1852
4	2-5	-4.038	0.1009	-5.2410	0.1700	-4.5166	0.1430	-4.4281	0.0933
5	3-4	2.787	0.0290	3.0382	0.0345	2.2238	0.0185	2.1963	0.0181
6	4-5	1.056	0.0042	2.3274	0.0203	1.5340	0.0088	1.4931	0.0084

Table V presents, the voltage magnitudes (VM) and voltage angles (VA) without FACT devices and with FACT devices. With TCSC placed in the line 4, the voltage magnitudes at Bus No. 1 and Bus No. 2 have improved. But, after placing TCPAR in line no. 3, voltages of Bus No. 1 and Bus No. 2 have reduced. Where as in the case of UPFC, voltage at Bus No. 1 improved to the specified value of 1.0 pu. At bus no. 2, voltage is improved by a large amount and nearly equal to 1.0 pu.

TABLE V
Bus voltage magnitude and angle with and without FACTS Device

Bus No	Without FACTs		TCSC in line-4		TCPAR in line-3		UPFC in line-3	
	VM(pu)	VA(p.u)	VM(p.u)	VA(p.u)	VM(p.u)	VA(p.u)	VM(p.u)	VA(p.u)
1	**0.974**	3.295	**0.984**	-1.417	**0.9455**	-3.9347	**1.0000**	-4.2204
2	**0.974**	-3.908	**0.998**	-1.435	**0.9549**	-4.3681	**0.9921**	-4.4736
3	1.05	4.138	1.05	5.770	1.05	4.0482	1.0500	3.9747
4	1.05	1.139	1.05	2.506	1.05	1.6537	1.0500	1.6096
5	1.05	0	1.05	0	1.05	0	1.0500	0.0000
6			0.954	-5.241	0.9867	-2.2867	0.9803	-2.2902

B. 14-bus test system

The 14-bus test system [38] consists of five generator buses, eleven load buses and twenty transmission lines shown in Figure 15. The line flow limit is set to 120 MW. Bus 1 is the reference bus. Base MVA for the system is considered as 100MVA.

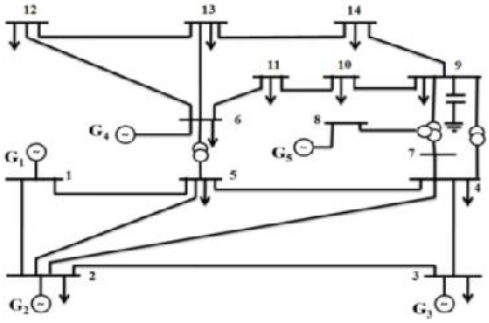

Fig. 15. 14-bus test system

The minimum and maximum limits of control parameters of FACT devices are presented in Table VI, for 14 bus system. Table VII, presents the optimal settings of the control parameters obtained with the help of N-R polar load flow solution. For obtaining the optimal parameter settings of FACT devices, on 14 bus system, same approach is followed as it was done in the case of 5 bus system.

TABLE VI
Limits of control parameters of FACTs devices

FACTs Device/Control parameter	TCSC	TCPAR	UPFC
X_{min} (p.u)	-0.3345	-	-
X_{max} (p.u)	0.3345	-	-
ϕ_{min} (deg)	-	-20^0	-
ϕ_{max} (deg)	-	20^0	-
V_{cR}^{min} (p.u)	-	-	0.001
V_{cR}^{max} (p.u)	-	-	0.3
V_{vR}^{min} (p.u)	-	-	0.9
V_{vR}^{max} (p.u)	-	-	1.1

TABLE VII
Optimal Setting of control parameters of FACTs devices

FACTs Device/Control parameter	TCSC	TCPAR	UPFC
X_C (p.u)	-0.1505	-	-
ϕ (deg)	-	15.61^0	-
θ_{cR} (deg)	-	-	98.59^0
θ_{vR} (deg)	-	-	-5.2498^0
V_{cR} (p.u)	-	-	0.2495
V_{vR} (p.u)	-	-	1.0252

For TCSC, optimal setting of reactance is - 0.1505p.u. For TCPAR, optimal shift in phase angle is 15.61^0. Series injected voltage of UPFC is, V_{cR} is obtained as $0.2495 \angle 98.59^0$ and voltage across the shunt converter is V_{vR} is obtained as $1.0252 \angle -5.2498^0$.

The optimal location for 14 bus system for each device is presented in the column 2 of Table 8. Real power loss before and after placing each device is presented in column 5. Real power flow performance index before and after placing FACTs device is presented in Column 6. Percentage reduction in PI is presented in Column 7. It is observed that, For 14 Bus System, with all devices, PI values have reduced and active power loss is slightly increased. In all the test systems, it is observed that power flows have been controlled as per the limits specified and voltage profile has been improved. Percentage reduction in PI is nearly same in all cases and is equal to 42.4%.

TABLE VIII
Real power loss, PI and % Reduction in PI value

FACTs Device	Line No	From Bus	To Bus	Real Power Loss	Performance Index	% reduction in PI value
System without any FACTs	-	-	-	0.1339	0.8462	-
TCSC	2	5	1	0.1461	0.4872	42.42
TCPAR	2	5	1	0.1462	0.4872	42.42
UPFC	2	5	1	0.1456	0.4871	42.44

Power flows before and after placing the three FACTS devices is presented in Table IX. Without any device, in 14 bus system, Line no.1 is observed to carry power flow of 1.5690 pu. For the NR power flow algorithm, maximum power flow is specified as 1.2 pu on all lines. It is observed that in all the three cases, the power flow is restricted to 1.125 pu in line no. 1 after placing the devices.

Table IX
Power flow results with and without FACTS Device

L.No	Fr-To	Without FACTs		TCSC in line-2		TCPAR in line-2		UPFC in line-2	
		Pline (p.u)	Ploss (p.u)	Pline (p.u)	Ploss (p.u)	Pline (p.u)	Ploss (p.u)	Pline (p.u)	Ploss (p.u)
1	1-2	**1.5690**	0.0430	**1.1256**	0.0219	**1.1258**	0.0219	**1.1251**	0.022
2	5-1	-0.7549	0.0276	**-1.1388**	0.0717	**-1.1388**	0.0715	**-1.1388**	0.072
3	2-3	0.7325	0.0232	0.6623	0.0191	0.0663	0.0191	0.6614	0.019
4	2-4	0.5628	0.0169	0.4130	0.0092	0.4130	0.0092	0.4130	0.009
5	2-5	0.4136	0.0090	0.2115	0.0029	0.2113	0.0029	0.2118	0.003
6	3-4	-0.2327	0.0037	-0.2988	0.0063	-0.2985	0.0064	-0.2996	0.006
7	4-5	-0.6247	0.0053	-0.8223	0.0097	-0.8217	0.0097	-0.8238	0.009
8	4-7	0.3002	0.0	0.2915	0.0	0.2913	0.0	0.2920	0.0
9	4-9	0.1679	0.0	0.1629	0.0	0.1628	0.0	0.1633	0.0
10	5-6	0.4570	0.0	0.4715	0.0	0.4718	0.0	0.4706	0.0
11	6-11	0.0644	0.0005	0.0726	0.0005	0.0728	0.0006	0.0722	0.001
12	6-12	0.0767	0.0007	0.0778	0.0007	0.0778	0.0007	0.0777	0.001
13	6-13	0.1728	0.002	0.1770	0.0021	0.1771	0.0021	0.1767	0.002
14	7-8	0.0	0.0	0.0	0.0	0.0	0.0	0.0	0.0
15	7-9	0.2936	0.0	0.2851	0.0	0.2849	0.0	0.2856	0.0
16	9-10	0.0612	0.0002	0.0532	0.0001	0.0530	0.0001	0.0536	0.001
17	9-14	0.1	0.0013	0.0948	0.0012	0.0947	0.0012	0.0952	0.001
18	10-11	-0.0289	0.0001	-0.0370	0.0001	-0.0371	0.0001	-0.0365	0.001
19	12-13	0.0150	0.0001	0.0160	0.0001	0.0161	0.0001	0.0159	0.001
20	13-14	0.0507	0.0005	0.0559	0.0005	0.0560	0.0005	0.0555	0.001

Table X presents, the voltage magnitudes (VM) and voltage angles (VA) without FACT devices and with FACT devices.

IV. CONCLUSION

In this paper, optimal parameter setting of FACTs devices has been carried out. Newton- Raphson (NR) power flow technique is used to determine the optimal parameter settings of TCSC, TCPAR and UPFC. The models of FACTs devices are presented and analyzed. The algorithm is implemented on standard 5 bus and 14 bus systems. Power loss and Performance Index values before and after placing the

Table X
Bus voltage magnitude and angle with and without FACTs Device

Bus	Without FACTs		TCSC in line-4		TCPAR in line-3		UPFC in line-3	
No	VM(p.u)	VA(p.u)	VM(p.u)	VA(p.u)	VM(p.u)	VA(p.u)	VM(p.u)	VA(p.u)
1	1.06	0	1.06	0	1.06	0	1.06	0
2	1.045	-4.9830	1.045	-3.5122	1.045	-3.51	1.045	-3.5104
3	1.01	-12.727	1.01	-10.476	1.01	-10.48	1.01	-10.465
4	1.0187	-10.343	1.0169	-7.3039	1.02	-7.29	1.0186	-7.3267
5	1.0208	-8.7770	1.017	-5.187	1.02	-5.17	1.02	-5.2342
6	1.07	-14.830	1.07	-11.454	1.07	-11.45	1.07	-11.472
7	1.0625	-13.668	1.06	-10.542	1.06	-10.53	1.0622	-10.562
8	1.09	-13.668	1.06	-10.542	1.09	-10.53	1.09	-10.562
9	1.0571	-15.316	1.05	-12.145	1.05	-12.14	1.0566	-12.166
10	1.0520	-15.515	1.05	-12.308	1.05	-12.30	1.0516	-12.329
11	1.0575	-15.303	1.05	-12.012	1.06	-12.00	1.0572	-12.032
12	1.0552	-15.668	1.05	-12.307	1.05	-12.30	1.0552	-12.325
13	1.0506	-15.733	1.05	-12.386	1.05	-12.38	1.0505	-12.404
14	1.0363	-16.496	1.04	-13.250	1.04	-13.24	1.036	-13.269
15			1.07	-14.290	0.99	-14.33	1.065	-14.290

FACTs device have been compared. It is observed that, for 5 Bus system, after placement of TCSC and TCPAR, the performance index is reduced but, power loss is slightly increased. But, in the case of UPFC, both performance index and real power loss have been reduced. For 14 Bus System, with all devices, PI values have reduced and active power loss is slightly increased. Power flow limit on all lines for 5 bus system is considered as 8.0 pu and 14 Bus system is 1.2 pu. In both the test systems, it is observed that power flows have been controlled as per the limits specified.

APPENDIX

The elements of Jacobian in equation (6), (12), and (31) are given as below:

TCSC–Partial derivatives of powers with respect to series compensator are:

$$\frac{\partial P_i}{\partial X_c} X_c = -V_i V_j B_{ij} \sin(\theta_i - \theta_j) \quad \text{A.1}$$

$$\frac{\partial Q_i}{\partial X_c} X_c = V_i^2 B_{ii} + V_i V_j B_{ij} \cos(\theta_i - \theta_j) \quad \text{A.2}$$

$$\frac{\partial P_j}{\partial X_c} X_c = -V_i V_j B_{ji} \sin(\theta_j - \theta_i) \quad \text{A.3}$$

$$\frac{\partial Q_j}{\partial X_c} X_c = V_j^2 B_{jj} + V_i V_j B_{ji} \cos(\theta_j - \theta_i) \quad \text{A.4}$$

$$\frac{\partial P_{ij}^c}{\partial X_c} X_c = -V_i V_j B_{ij} \sin(\theta_i - \theta_j) \quad \text{A.5}$$

TCPAR–Partial derivatives of powers with respect to phase angle shift of TCPAR, bus voltage magnitudes and voltage angles.

$$\frac{\partial P_i}{\partial \theta_i} = -\frac{\partial P_i}{\partial \theta_j} = -\frac{\partial Q_i}{\partial V_j} V_j = -\frac{\partial P_i}{\partial \alpha} = -Q_i - V_i^2 B_{ii} \quad \text{A.6}$$

$$\frac{\partial P_i}{\partial V_i} V_i = P_i + V_i^2 G_{ii} \quad \text{A.7}$$

$$\frac{\partial Q_i}{\partial \theta_i} = -\frac{\partial Q_i}{\partial \theta_j} = -\frac{\partial P_i}{\partial V_j} V_j = -\frac{\partial Q_i}{\partial \alpha} = P_i - V_i^2 G_{ii} \quad \text{A.8}$$

$$\frac{\partial Q_i}{\partial V_i} V_i = Q_i - V_i^2 B_{ii} \quad \text{A.9}$$

$$\frac{\partial Pj}{\partial \theta_j} = -\frac{\partial P_j}{\partial \theta_i} = -\frac{\partial Q_j}{\partial V_i} V_i = \frac{\partial P_j}{\partial \alpha} = -Q_j - V_j^2 B_{jj} \quad \text{A.10}$$

$$\frac{\partial Pj}{\partial V_j} V_j = P_j + V_j^2 G_{jj} \quad \text{A.11}$$

$$\frac{\partial Q_j}{\partial \theta_j} = -\frac{\partial Q_j}{\partial \theta_i} = \frac{\partial Pj}{\partial V_i} V_i = \frac{\partial Q_i}{\partial \alpha} = P_j - V_j^2 G_{jj} \quad \text{A.12}$$

$$\frac{\partial Q_j}{\partial V_j} V_j = Q_j - V_j^2 B_{jj} \quad \text{A.13}$$

It should be noted that since $P^s_{ij}=P_i$, the following relations hold true and simplify the evaluation of the Jacobian matrix,

$$\frac{\partial P^s_{ij}}{\partial \theta_i} = \frac{\partial P_i}{\partial \theta_i} \quad \text{A.14}$$

$$\frac{\partial P^s_{ij}}{\partial \theta_j} = \frac{\partial P_i}{\partial \theta_j} \quad \text{A.15}$$

$$\frac{\partial P^s_{ij}}{\partial V_i} V_i = \frac{\partial P_i}{\partial V_i} V_i \quad \text{A.16}$$

$$\frac{\partial P^s_{ij}}{\partial V_j} V_j = \frac{\partial P_i}{\partial V_j} V_j \quad \text{A.17}$$

$$\frac{\partial P^s_{ij}}{\partial \alpha} = \frac{\partial P_i}{\partial \alpha} \quad \text{A.18}$$

UPFC–Partial derivatives of powers, with respect to voltage magnitudes and angles of shunt and series converters are.

At bus i is:

$$\frac{\partial P_i}{\partial \theta_i} = -Q_i - V_i^2 B_{ii} \quad \text{A.19}$$

$$\frac{\partial Q_i}{\partial \theta_i} = P_i - V_i^2 G_{ii} \quad \text{A.20}$$

$$\frac{\partial P_i}{\partial \theta_j} = V_i V_j [G_{ij} \sin(\theta_i - \theta_j) - B_{ij} \cos(\theta_i - \theta_j)] \quad \text{A.21}$$

$$\frac{\partial Q_i}{\partial \theta_j} = -V_i V_j [G_{ij} \cos(\theta_i - \theta_j) + B_{ij} \sin(\theta_i - \theta_j)] \quad \text{A.22}$$

$$\frac{\partial P_i}{\partial V_i} V_i = P_i + V_i^2 G_{ii} \quad \text{A.23}$$

$$\frac{\partial Q_i}{\partial V_j} V_j = V_i V_j [G_{ij} \sin(\theta_i - \theta_j) - B_{ij} \cos(\theta_i - \theta_j)] \quad \text{A.24}$$

$$\frac{\partial P_i}{\partial V_j} V_j = V_i V_j [G_{ij} \cos(\theta_i - \theta_j) + B_{ij} \sin(\theta_i - \theta_j)] \quad \text{A.25}$$

$$\frac{\partial Q_i}{\partial V_i} V_i = Q_i - V_i^2 B_{ii} \quad \text{A.26}$$

$$\frac{\partial P_i}{\partial \phi_{cR}} = V_i V_{cR} [G_{ij} \sin(\theta_i - \phi_{cR}) - B_{ij} \cos(\theta_i - \phi_{cR})] \quad \text{A.27}$$

$$\frac{\partial Q_i}{\partial \phi_{cR}} = -V_i V_{cR} [G_{ij} \cos(\theta_i - \phi_{cR}) + B_{ij} \sin(\theta_i - \phi_{cR})] \quad \text{A.28}$$

$$\frac{\partial P_i}{\partial V_{cR}} V_{cR} = V_i V_{cR} [G_{ij} \cos(\theta_i - \phi_{cR}) + B_{ij} \sin(\theta_i - \phi_{cR})] \quad \text{A.29}$$

$$\frac{\partial Q_i}{\partial V_{cR}} V_{cR} = V_i V_{cR} [G_{ij} \sin(\theta_i - \phi_{cR}) - B_{ij} \cos(\theta_i - \phi_{cR})] \quad \text{A.30}$$

$$\frac{\partial P_i}{\partial \phi_{vR}} = V_i V_{vR} [G_{ij} \sin(\theta_i - \phi_{vR}) - B_{ij} \cos(\theta_i - \phi_{vR})] \quad \text{A.31}$$

$$\frac{\partial Q_i}{\partial \phi_{vR}} = -V_i V_{vR} [G_{ij} \cos(\theta_i - \phi_{vR}) + B_{ij} \sin(\theta_i - \phi_{vR})] \quad \text{A.32}$$

$$\frac{\partial P_i}{\partial V_{vR}} V_{vR} = V_i V_{vR} [G_{ij} \cos(\theta_i - \phi_{vR}) + B_{ij} \sin(\theta_i - \phi_{vR})] \quad \text{A.33}$$

$$\frac{\partial Q_i}{\partial V_{vR}} V_{vR} = V_i V_{vR} [G_{ij} \sin(\theta_i - \phi_{vR}) - B_{ij} \cos(\theta_i - \phi_{vR})] \quad \text{A.34}$$

At bus j is:

$$\frac{\partial P_j}{\partial \theta_i} = V_i V_j [G_{ji} \sin(\theta_j - \theta_i) - B_{ji} \cos(\theta_j - \theta_i)] \quad \text{A.35}$$

$$\frac{\partial P_j}{\partial \theta_j} = -Q_j - V_j^2 B_{jj} \quad \text{A.36}$$

$$\frac{\partial Q_j}{\partial \theta_j} = P_j - V_j^2 G_{jj} \quad \text{A.37}$$

$$\frac{\partial P_j}{\partial V_i} V_i = V_i V_j [G_{ji} \cos(\theta_j - \theta_i) + B_{ji} \sin(\theta_j - \theta_i)] \quad \text{A.38}$$

$$\frac{\partial Q_j}{\partial V_i} V_i = V_i V_j [G_{ji} \sin(\theta_j - \theta_i) - B_{ji} \cos(\theta_j - \theta_i)] \quad \text{A.39}$$

$$\frac{\partial P_j}{\partial V_j} V_j = P_j + V_j^2 G_{jj} \quad \text{A.40}$$

$$\frac{\partial Q_j}{\partial V_j} V_j = Q_j - V_j^2 B_{jj} \quad \text{A.41}$$

$$\frac{\partial P_j}{\partial \phi_{cR}} = V_j V_{cR} [G_{jj} \sin(\theta_j - \phi_{cR}) - B_{jj} \cos(\theta_j - \phi_{cR})] \quad \text{A.42}$$

$$\frac{\partial Q_j}{\partial \phi_{cR}} = -V_j V_{cR} [G_{jj} \cos(\theta_j - \phi_{cR}) + B_{jj} \sin(\theta_j - \phi_{cR})] \quad \text{A.43}$$

$$\frac{\partial P_j}{\partial V_{cR}} V_{cR} = V_j V_{cR} [G_{jj} \cos(\theta_j - \phi_{cR}) - B_{jj} \sin(\theta_j - \phi_{cR})] \quad \text{A.44}$$

$$\frac{\partial Q_j}{\partial V_{cR}} V_{cR} = V_{cR} V_j [G_{jj} \sin(\theta_j - \phi_{cR}) - B_{jj} \cos(\theta_j - \phi_{cR})] \quad \text{A.45}$$

At the UPFC series converter is:

$$\frac{\partial P_{cR}}{\partial \theta_i} = V_i V_{cR} [G_{ij} \sin(\phi_{cR} - \theta_i) - B_{ij} \cos(\phi_{cR} - \theta_i)] \quad \text{A.46}$$

$$\frac{\partial P_{cR}}{\partial \phi_{cR}} = -Q_{cR} - V_{cR}^2 B_{jj} \quad \text{A.47}$$

$$\frac{\partial P_{cR}}{\partial \theta_j} = V_j V_{cR}[G_{jj}\sin(\phi_{cR} - \theta_j) - B_{jj}\cos(\phi_{cR} - \theta_j)] \quad \text{A.48}$$

$$\frac{\partial P_{cR}}{\partial V_{cR}} V_{cR} = P_{cR} + V_{cR}^2 G_{jj} \quad \text{A.49}$$

$$\frac{\partial P_{cR}}{\partial V_i} V_i = V_i V_{cR}[G_{ij}\cos(\phi_{cR} - \theta_i) + B_{jj}\sin(\phi_{cR} - \theta_i)] \quad \text{A.50}$$

$$\frac{\partial P_{cR}}{\partial V_j} V_j = V_j V_{cR}[G_{jj}\cos(\phi_{cR} - \theta_j) + B_{jj}\sin(\phi_{cR} - \theta_j)] \quad \text{A.51}$$

At the UPFC shunt converter is:

$$\frac{\partial P_{vR}}{\partial \theta_i} = V_i V_{vR}[G_{vR}\sin(\phi_{vR} - \theta_i) - B_{vR}\cos(\phi_{vR} - \theta_i)] \quad \text{A.52}$$

$$\frac{\partial P_{vR}}{\partial \phi_{vR}} = -Q_{vR} - V_{vR}^2 B_{vR} \quad \text{A.53}$$

$$\frac{\partial P_{vR}}{\partial V_i} V_i = V_i V_{vR}[G_{vR}\cos(\phi_{vR} - \theta_i) + B_{vR}\sin(\phi_{vR} - \theta_i)] \quad \text{A.54}$$

$$\frac{\partial P_{vR}}{\partial V_{vR}} V_{vR} = P_{vR} + V_{vR}^2 G_{vR} \quad \text{A.55}$$

REFERENCES

[1] S. N. Singh and A. K. David, "Congestion Management by Optimizing FACTS Device Location," *Proc. of International conference on Electric utility deregulation & restructuring and power technologies 2000*, City university, London, 4-7 April 2000,pp. 23-28.

[2] N. G. Hingorani, "High power electronics and flexible AC transmission system," IEEE Power Engineering review, july 1988.

[3] S. N. Singh, "Location of FACTS devices for enhancing power systems' security", *The 2001 Large Engineering Systems Conference on Electrical Power Engineering* (LESCOPE), Halifax, Nova Scotia, Canada, pp 162-166, July 11-13, 2001

[4] K. R. Padiyar "*FACTS controllers in power transmission and distribution*", New Age International (P) Ltd., 2007.

[5] L. Gyugyi, "A unified power flow control concept for flexible AC transmission systems", *IEE Proc., Pail-C*, vol. 139, No.4, pp. 323-331, July 1992.

[6] E. Larsen, N. Miller, S. Nilsson and S. Lindgren, "Benefits of GTO Based compensation systems for electric utility applications*"*, *IEEE Trans. on Power Delivery*, vol. 7, no. 4, pp. 2056- 2064, Oct. 1992.

[7] M. Noroozian and G. Anderson, "Power flow control by use of controllable series components", *IEEE Trans. on Power Delivery*, vol. 8, no. 3, pp. 1420-1429, July 1993.

[8] S. Gerbex, R. Cherkaoui, and A. Germond, "Optimal location of multitype FACTS devices in a power system by means of genetic algorithms," *IEEE Transaction Power System*, vol. 16, no. 3, pp. 537-544, Aug. 2001.

[9] N. Sharma, A. Ghosh, and R. Varma, "A novel placement strategy for FACTS controllers," *IEEE Transaction Power Delivery*, vol. 18, pp. 982-987, July 2003.

[10] J. G. Singh, S. N. Singh, and S. C. Srivastava, "Placement of FACTS controllers for enhancing power system loadability," *IEEE power India conference*, New Delhi, 2006.

[11] P. Preedavichit and S. C. Srivastava, "Optimal reactive power dispatch considering FACTS devices", *Electric Power Systems Research*, vol. 46, no. 3, pp. 251-257, Sept. 1998.

[12] R. S. Fang, A. K. David, "Transmission Congestion Management in an Electricity Market", *IEEE Transactions on Power Systems*, vol. 14, no. 3, pp. 877- 883, Aug. 1999.

[13] N. Acharya, N. Mithulanathan, "Locating Series FACTS devices for Congestion Management in Deregulated Electricity Markets", *Electric Power Systems Research*, vol. 77, no. 3-4, pp. 352-360, March 2007.

[14] J. Brosda, E. Handschin, "Congestion Management Methods with a Special Consideration of FACTS-Devices", *IEEE Power Tech2001 Porto*, vol. 1, 10-13, Sept. 2001.

[15] A. A. Athamneh, W. J. Lee, "Benefits of FACTS devices for power exchange among Jordanian Interconnection with other Countries", *Power Engineering Society General Meeting*, June 2006.

[16] S. N. Singh and S. C. Srivastava, "Corrective action planning to achieve a feasible optimum power flow solution", *IEE Proc. Part-C*, vol. 142, no. 6, pp. 576 -582, Nov. 1995

[17] G.D. Galiana et al, "Assessment and control of the impact of FACTS devices on power system performance", *IEEE Trans on Power System*, vol. 11, no. 4, pp. 1931-1936, Nov. 1996.

[18] R. Rajaraman, F. Alvarado, A. Maniaci, R. Camfield and S. Jalali, "Determination of location and amount of series compensation to increase power transfer capability", *IEEE Trans. on Power Systems*, vo1.13, no.2, pp. 294-299, May 1998.

[19] E.J. de Oliveira and J.W.M. Lima, "Allocation of FACTS devices in a competitive environment", *13th PSCC*, 1999, pp. 1184-1 190.

[20] M. Adamiak and R. Patterson, "Protection requirements for flexible AC transmission systems", in *Proc. CIGRE*, Paris, France, 1992.

[21] Y. H. Song and A. T. Johns, *Flexible AC Transmission Systems (FACTS)*, U.K. IEE, 1999, ch. 12.

[22] A. Girgis, A. Sallam, and A. K. El-Din, "An adaptive protection scheme for advanced series compensated (ASC) transmission lines", *IEEE Trans. Power Del.*, vol. 13, no. 2, pp. 414–420, Apr. 1998.

[23] W. Weiguo *et al.*, "The impact of TCSC on distance protection relay", in *Proc. Int. Conf. Power System Technol.*, vol. 1, Aug. 18–21, 1998, pp. 382–388.

[24] L. Gyugyi, C.D. Shauder, S.L.Williams, T.R. Rietman, D.R.Torgerson, and A. Edris, "The unified power flow controller: a new approach to power transmission control", IEEE Trans. Power Deli., Vol. 10, No. 2, pp.1085-1097, Oct. 1995.

[25] I. Marouani, T. Guesmi, H.H. Abdallah, A. Ouali, "Application of a multi-objective evolutionary algorithm for optimal location and parameters of FACTS devices considering the real power loss in transmission lines and voltage deviation buses", Proceedings of the 6th International Multi-Conference on Systems, Signals and Devices, 23rd -26th March 2009, pp. 1-6.

[26] Q. H. Wu, Z. Lu, M.S. Li, T.Y. Ji, "Optimal placement of FACTS devices by a group search optimizer with multiple producer", Proceedings of the IEEE Congress on Evolutionary Computation, 1st -6th June 2008, pp. 1033-1039.

[27] H. Mori, and Y. Goto, "A Parallel Tabu Search Based Method for Determining Optimal Allocation of FACTS in Power Systems", Proc. of Int. Conf. on Power System Technology PowerCon, 4th -7th December 2000, vol. 2, pp. 1077- 1082.

[28] F. G. M. Lima, F. D. Galiana, I. Kockar, and Jorge Munoz, "Phase Shifter Placement in Large Scale Systems via Mixed Integer Linear Programming", IEEE Trans. on Power Systems, vol. 18, no. 3, pp. 1029-1034, Aug. 2003.

[29] H. Sawhney and B. Jeyasurya, "Application of Unified Power Flow Controller for Available Transfer Capability Enhancement", Electric Power Systems Research, Vol. 69, No. 2-3, pp. 155-160, May 2004.

[30] E. V. Larsen, K. Clark, S. S. Miske and J. Urbanek, "Characteristics and Rating Considerations of Thyristor Controlled Series Compensation", IEEE *Trans. on Power Delivery*, Vol. 9, No. 2, pp. 992-1000, April 1994.

[31] E. Larsen, C. Bowler, B. Damsky and S. Nilsson, "Benefits of Thyristor Controled Series Compensation", International Conference on Large High Voltage Electric Systems (CIGRÉ), paper 14/37/38-04, Paris, September 1992.

[32] W. F. Tinney and J. M. Walker, "Direct Solutions of Sparse Network Equations by Optimally Ordered Triangular Factorization", *Proceedings of* IEEE, Vol. 55, pp. 1801-1809, November 1967.

[33] G. W. Stagg and A.H. El-Abiad, "Computer Methods in Power System Analysis", McGraw-Hill, 1968.

[34] IEEE Power Engineering Society/CIGRÉ, "FACTS Overview", Special Issue, 95TP108, IEEE Service Center, Piscataway, N.J., 1995.

[35] R. J. Nelson, "Transmission Power Flow Control: Electronic vs. Electromagnetic Alternatives for Steady-State Operation", IEEE *Trans. on Power Delivery*, Vol. 9, No. 3, pp. 1678-1684, July 1994.

[36] A. Nabavi-Niaki and M. R. Iravani, "Steady-State and Dynamic Models of Unified Power Flow Controller (UPFC) for Power System Studies", Presented at 1996 IEEE/PES Winter Meeting, 96 WM 257-6 PWRS, January 21-25, 1996, Baltimore, MD.

[37] Antonio Gomez- Exposito, Antonio J. Conejo, and Claudio Canizares, "*Electric Energy Systems Analysis and Operation*", CRC Press, New York, 2009.

[38] L. L. Freris and A. M. Sasson, "Investigation of the Load Flow Problem", *Proc IEE*, vol. 115, No. 10, pp. 1459-1469, October 1968.

[39] V. Srinivasa Rao and R. Srinivasa Rao, "Comparison of Various Methods for Optimal Placement of FACT Devices", *Smart Electric Grid (ISEG), 2014 IEEE International Conference on*, pp. 1-7, 19-20 Sept. 2014.

[40] R. Srinivasa Rao and V. Srinivasa Rao, "A generalized approach for determination of optimal location and performance analysis of FACT devices", International Journal of Electrical Power and Energy Systems, Vol.73, pp. 711-724, 2015.